

Mass transport in carbon gels with tuned porosity

Transferencia de masa en geles de carbón con porosidad a medida

N. Job*

University of Liège, Laboratory of Chemical Engineering B6a, Sart-Tilman, B-4000 Liège, Belgium.

*Corresponding author: Nathalie.Job@ulg.ac.be

Abstract

Diffusional limitations in carbon gel-supported catalysts are often encountered despite their open structure. However, the analysis of mass transport is rarely taken into account in studies dealing with catalyst preparation and test using these nanostructured carbons as supports. Any catalytic system should be first subject to mass transport analysis before any conclusion can be drawn about relationships between the physico-chemical properties and the measured activity of the catalyst.

Resumen

Pese a su estructura abierta, a menudo se observan limitaciones difusionales en catalizadores soportados en geles de carbono. Sin embargo, en los diversos estudios de preparación y testeo de catalizadores soportados en estos materiales nanoestructurados, pocas veces se lleva a cabo un análisis de transferencia de masa. Así, antes de obtener cualquier conclusión sobre la relación entre las propiedades fisicoquímicas y la actividad de un catalizador, el sistema debería someterse a un análisis de transporte de masa.

1. Introduction

Porous carbon materials are widely used in many applications: adsorption in liquid or gas phase, gas separation, supports for catalysts, electrocatalysis, materials for batteries, etc. In all these processes, the pore texture of the chosen carbon material plays a major role. Indeed, whatever the above-mentioned application, species which can be adsorbates, reactants or ions must circulate within the pore texture. The control of the carbon pore texture is thus key to an efficient process.

However, carbons used in industrial applications or in electrochemical devices, such as activated carbons or carbon blacks, most often display quite inappropriate pore textures with regard to mass transport. The texture of activated carbons, for instance, is generally microporous, with low macropore or mesopore volumes, which often induces diffusional limitations during catalytic and

adsorption processes. Carbon blacks, which are composed of microporous near-spherical particles of colloidal sizes ($\sim 20 - 60$ nm), coalesced together as aggregates ($1 - 100$ μm), remain the elected material for Proton Exchange Membrane fuel cell electrodes [1]; however, the pore texture of the electrodes is quite dependant on the electrode processing because it is to a large extent defined by the packing of the carbon aggregates, which depends on the electrode manufacture technique.

These drawbacks call for the development of carbon materials with controllable and tunable pore texture. This is why so many recent works were dedicated to the preparation of synthetic porous carbon materials, with special attention to the control of the textural properties. Several routes were investigated in the last 20 years and, among the numerous new carbon materials developed, carbon gels, *i.e.* carbon xerogels, aerogels and cryogels, have been successfully used at laboratory scale as alternative to commercial carbons in several processes. The advantage of carbon gels is that their pore texture, *i.e.* pore size and pore volume, can be very accurately tuned within a wide range. As a result, one can adapt the pore texture of the used carbon with regard to the application in order to get rid of diffusional limitations encountered with mainly microporous materials. However, the elimination of mass transport limitations is not straightforward since it does not only depend on the pore size, but also on the void fraction, on the tortuosity of the pores and on the characteristic dimension of the catalyst pellet or particle. The aim of the present paper is to highlight the advantages of these materials in terms of mass-transport control, and to underline the precautions to be taken when using these *a priori* "diffusional limitation-free" materials.

2. Preparation of carbon gels with tuned pore texture

The preparation of carbon gels and the final pore texture obtained in function of the preparation recipe used is very well referenced in the literature [2]. Although alternatives can be found, most studies report the mixing of resorcinol and formaldehyde

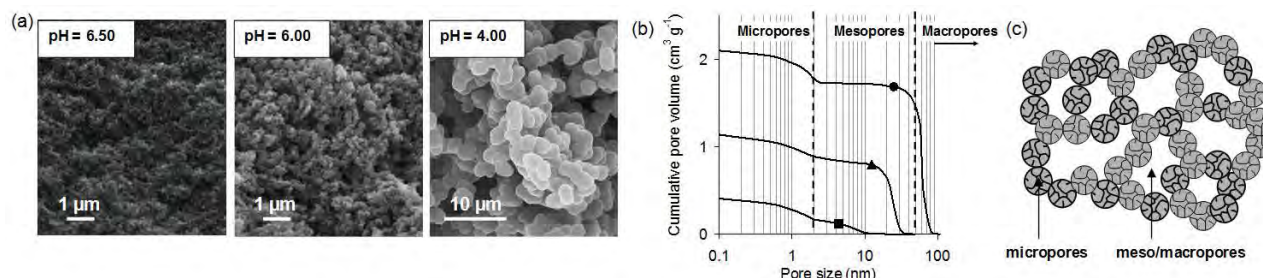


Figure 1. (a) Scanning electron micrographs of three carbon xerogels prepared at the same dilution ratio ($D = 5.7$) and various pH conditions. (b) Pore size distribution of carbon xerogels ($D = 5.7$) prepared at pH = 5.25 (\bullet), pH = 5.75 (\square) and pH = 6.25 (\triangle). (c) Carbon gel modeling: covalently bonded microporous spherical-like nodules separated by meso/macropores. **Figura 1.** Micrografías electrónicas de barrido de tres xerogeles de carbón preparados con la misma relación de dilución ($D = 5.7$) y diferentes pHs. (b) Distribución del tamaño de poros de xerogeles de carbón ($D = 5.7$) preparados a pH = 5.25 (\bullet), pH = 5.75 (\square) and pH = 6.25 (\triangle). (c) Modelo de gel de carbón: nódulos esféricos microporosos enlazados covalentemente separados por meso/macroporos.

(reagents) in water (solvent) and use of sodium carbonate as basification agent (also called 'base catalyst'). After gelation and ageing, the gel is composed of interconnected spherical nodules delimiting voids filled with the solvent. After drying and pyrolysis, the so-called 'string-of-pearl'-like structure remains (Fig. 1a) whatever the drying technique, although large variations in the final pore volume can be observed depending on the method used (evaporation, supercritical drying or freeze-drying). Pyrolysis induces the development of microporosity within the nodules. As a result, carbon gels display a bimodal pore texture (Fig. 1b): meso/macropores are delimited by the spacing between microporous nodules (Fig. 1c).

In order to change (tune) the pore texture of the final material, one can play on three main variables [3]: (i) the pH of the precursor solution, (ii) the dilution ratio, *i.e.* the water/reactants molar ratio and (iii) the drying technique. In a global way, the nodule size is mainly fixed by the pH of the precursor solution while the pore volume and pore size are mostly related to the dilution ratio and drying technique. However, the relationship between the synthesis/drying variables and the pore texture parameters is not straightforward. The dilution ratio, for instance, also impacts the nodule size, although to a less extent than the pH of the solution. The nature and concentration of ions also modifies the texture: for instance, adjusting two gels at the same pH with NaOH or Mg(OH)₂ leads to two different materials [4]. The drying technique impacts strongly the pore texture when the pores are small and when the dilution ratio is high. Indeed, in this case, evaporation leads to a shrunk material with low pore volume compared to materials obtained by supercritical drying or freeze-drying. However, as the solid fraction and pore size increases, capillary tensions induced by the curved liquid-vapor interface during evaporation decreases, and no shrinkage is observed whatever the drying technique [3]. Finally, the pore size and pore volume of carbon gels can be tuned independently within a wide range: from a few nm to a few μm , and from 0 to 5–6 cm^3/g , respectively. This leaves plenty of room for adjustment with regard to the final application.

3. Use in mass-transport dependant processes

3.1. Heterogeneous catalysis

The deposition of active species on carbon gels is not more difficult than in the case of other carbon supports, but one of the advantages is that the surface chemistry can also be tuned by post-treatments [5], which further eases the impregnation with metal precursors for instance, or even the grafting of metal complexes. Many studies have reported the preparation of metal, alloy or oxide catalytic nanoparticles on such supports and their use in various catalytic processes [6]. However, few of them include the analysis of mass transport limitations in their discussion of results and, due to the lack of appropriate data, it is often difficult to determine whether the measured activity of the catalyst is diffusion-free or not. The danger here is to attribute reaction rate constancy or modifications to the physico-chemical characteristics of the catalyst (e.g. composition, surface chemistry, dispersion, etc.) while the system is in fact dominated by mass transport effects: in this case, the measured reaction rate is not the *specific* reaction rate, *i.e.* related to the physico-chemical properties of the catalytic sites, but an *apparent* reaction rate, somewhat falsified by mass-transport limitations.

This problem is quite classical in heterogeneous catalysis (Fig. 2) [7]: to reach the catalytic sites, reactants have first to diffuse through an external stagnant film of fluid outside the catalyst pellet and must then circulate within the pores of the support; products must then go the reverse way. In the case the reaction is intrinsically slow and the mass transport is fast enough, the concentration of reactants and products is quite homogeneous everywhere (Fig. 2a: *chemical regime*). However, when the kinetics of the reaction is fast and the diffusion rate is slow, a concentration gradient appears in the catalyst pellet and/or in the external stagnant film outside the pellet (Fig. 2b: *diffusional regime*). As a result, the reactant concentration at the catalytic site, C , which generally affects the kinetics of the reaction, is not that measured outside the catalyst pellet, C_e : the reaction rate measured by the experimenter is a mix between various reaction rates because each catalytic site actually 'sees' a different concentration of reactants (and products). Another consequence is that catalytic sites located at the pellet centre are almost useless because they are not reached by the reactants. The ratio between this *apparent* reaction rate, r_a , and the *specific* reaction rate, r_s , is called the *effectiveness factor* of the catalyst, η . This factor quantifies the gap between the true reaction kinetics over the catalytic sites and the reaction kinetics observed, which depends on the diffusion rate of the reactants and products in the external layer and within the pore texture of the support.

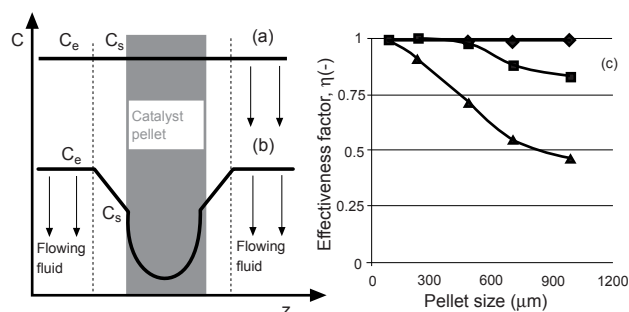


Figure 2. Mass transport in a catalyst pellet. (a) Reactant concentration profile in the case of *chemical regime*. (b) Reactant concentration profile in *diffusional regime*. C_e and C_s represent the concentration of a reactant in the flowing fluid and at the surface of the pellet, respectively. (c) Hydrodechlorination of 1,2-dichloroethane into ethylene on Pd-Ag/carbon xerogel catalysts, $T = 573\text{K}$. Effectiveness factor, η , as a function of the pellet size. Average pore size of the support: (p) ~10 nm, (n) ~30 nm, (u) ~70 nm. Data adapted from [8].

Figura 2. Transferencia de masa en una partícula de catalizador. (a) Perfil de concentración del reactivo en el caso de *régimen químico*. (b) Perfil de concentración del reactivo en *régimen difusional*. C_e and C_s representan la concentración del reactivo en el flujo y en la superficie de la partícula, respectivamente. (c) Hidrodecloración de 1,2-dicloroetano en etileno sobre catalizadores de Pd-Ag/xerogel de carbón, $T = 573\text{K}$. Factor de efectividad, η , en función del tamaño de partícula. Tamaño medio de poro del soporte: (p) ~10 nm, (n) ~30 nm, (u) ~70 nm. Datos adaptados de [8].

3.2. Determination of the external and internal limitations

In the case of carbon gels, like for any other porous material, selecting supports with 'large pores' does not necessarily mean that no diffusional problems will occur. As an example, Fig.2b shows the effectiveness factor of Pd-Ag catalysts supported on carbon xerogels with various meso/macropore

size in the case of hydrodechlorination of 1,2-dichloroethane into ethylene performed in gas phase at 573K [8]. One can observe that supports with small pore size lead to a rapid decrease of η , even with quite small pellets (500 μm). Larger pore sizes allow keeping the effectiveness factor equal to 1 for pellets of larger size (up to 7 mm by calculation in the case of 70 nm pores). Since too small pellets piled up in a reactor would lead to prohibitive pressure drop in the device, the possibility to use large pellets without loss of catalyst performance is obviously an advantage brought by an adequate pore texture of the support. However, increasing the temperature at 623K leads to internal diffusion limitations for pellets around 4 mm [8].

As a matter of fact, it is impossible to tell without any calculations or additional measurements whether kinetics is observed in chemical regime or not. So, before any discussion of the catalytic properties of carbon gel-supported catalysts, one must check that the obtained kinetics data are mass transport-free. In a practical way, *external limitations* can be detected by modifying the fluid flow rate (in the case of a continuous tubular reactor) or by changing the stirring speed (in the case of a continuous or discontinuous mixed reactor): these variables affect the thickness of the limit layer outside the catalyst pellet. *Internal limitations* can be detected by changing the pellet size: indeed, using smaller pellets obtained by grinding of larger ones would lead to a shorter average distance between the pellet surface and the catalytic sites and thus to a less severe internal concentration gradient. Note however that modifying the pellet size also decreases the thickness of the external film: so, the detection of internal limitations must be performed in the absence of external limitations.

If the catalytic properties of a sample are not independent of the flow rate or mixing and pellet size, the obtained data are not specific to the physico-chemical properties of the catalyst itself but are relevant to fluid dynamics. It is thus completely illusory to link any of the catalyst properties to the observed reaction rate. Additional measurements are not always easy to perform, but the presence of external or internal limitations can be deduced from calculation. The external diffusional limitations can be quantified by the fraction of external resistance f_e [7]:

$$(1) \quad f_e = 1 - \frac{C_s}{C_e} = \frac{r_a L_p}{k_d C_e}$$

where r_a is the apparent specific reaction rate per volume unit of catalyst, L_p is the characteristic dimension of the catalyst pellet (*i.e.*, the volume to surface ratio, equal to $d_p/6$ in the case of a sphere, d_p being the pellet diameter), C_e and C_s are the concentration of the limiting reactant in the bulk of the fluid phase and at the external surface of the catalytic pellet, respectively, and k_d is the external transfer coefficient. k_d can be estimated from correlations between the Sherwood (Sh), Reynolds (Re) and Schmidt (Sc) dimensionless numbers [7]. Indeed:

$$(2) \quad Sh = \frac{k_d d_p}{D_m} = Sh_0 + B Re^m Sc^{\frac{1}{3}} = Sh_0 + B \left(\frac{\rho u d_p}{\mu} \right)^m \left(\frac{\mu}{\rho D_m} \right)^{\frac{1}{3}}$$

where Sh_0 is the Sherwood number in the absence of forced convection, D_m is the molecular diffusivity, d_p is the particle diameter, ρ , μ and w are respectively the density, the viscosity and the linear velocity of the fluid phase and B is a constant. In the case of a stirred reactor, the velocity of the fluid phase is calculated from the stirring speed of the reactor [7]. Specific correlations of the Eq. (2) form are available for many systems and under various conditions. All the parameters of these equations are characteristics of the fluid phase, reactor and catalyst pellet, which are normally accessible to the experimenter. The calculation of Sh and thus of f_e should not be a problem for usual reactors. Finally, if f_e is close to 1, one can conclude that no external limitations occur.

A quantitative approach to evaluate the influence of internal diffusion on the overall catalytic process consists in the calculation of the dimensionless Weisz modulus, ϕ , which is defined as the ratio between the apparent specific reaction rate and the diffusion rate of the reactant in the pore texture of the catalyst particle. For ϕ larger than 1, the internal diffusion limitations become rate-determining, and the observed reaction rate is falsified by mass transport within the pore texture. The Weisz modulus can be written as [7]:

$$(3) \quad \phi = \frac{r_a L_p^2}{D_e C_s}$$

where r_a is the apparent reaction rate per volume unit of catalyst, L_p is the characteristic dimension of the catalyst pellet, C_s is the concentration of the limiting reactant at the external particle surface, and D_e is the effective diffusivity through the catalyst pores. C_s is not easily determined unless the catalytic measurements are performed in the absence of external limitations, which is the usual way to proceed: in this case $C_s = C_e$. The effective diffusivity, D_e , is the diffusivity in the pores, D , corrected by the accessible void fraction, ε , and the pore tortuosity, τ [7]:

$$(4) \quad D_e = \frac{\varepsilon D}{\tau}$$

In liquid phase, D is the molecular diffusivity, D_m , available in tables. In gas phase and when the pores are small (typically < 100 nm), D is a combination of the both the molecular and the Knudsen diffusivities [9], the latter mechanism being related to diffusion in which collisions with the pore walls are predominant with regard to collisions between molecules. As a consequence, in Knudsen-type regime, the diffusivity changes with the pore size, which is not the case in molecular-type diffusion. Note also that the tortuosity of the catalyst support, τ , is often taken equal to $1/\varepsilon$.

3.3. Heterogeneous catalysis on carbon gels

The case of carbon gels is more complicated since one clearly identifies two pore levels (Fig. 1b-c). Indeed, internal limitations could occur either at the meso/macropore level or at the micropore level if the catalytic species are located in the microporosity. With this particular double structure of granular pellet itself composed of porous spheres, one can imagine to perform the internal mass transport analysis at both levels, *i.e.* by calculating the Weisz modulus at the pellet (ϕ_p) and at the nodule (ϕ_n) level [8]. All parameters related to the solid must then be those related either to the pellet or to the nodule. For

instance, the characteristic dimension L_p and the void fraction ε are different when considering each level. In particular, the void fraction of the nodules is almost constant (~ 0.35) because the structure of the nodules and thus their microporosity is quite independent on the synthesis conditions of the pristine gel, unless the carbon gel is further activated to develop its specific surface area [10]; on the contrary, the void fraction of carbon gel monoliths strongly depends on the synthesis and drying pathway (see §2). As an example, the Weisz modulus was calculated at the pellet and nodule levels for Pd-Ag catalysts supported on carbon xerogels of various pore textures [8], and it was clearly demonstrated that, when present, the diffusional limitations occur at the meso/macropore level and not in the micropores. This can be explained by the difference of distance to be covered by the molecules in the meso/macropores ($\sim 500 \mu\text{m}$ for 1 mm pellets) compared to micropores ($\sim 10 - 100 \text{ nm}$) to reach the centre of either the pellet or the nodule; this clearly demonstrates that the pore size is not the only factor to be taken into account.

Another source of complication is the fact that the catalytic species may be not homogeneously dispersed in the porosity of the support. For instance, the active particles can be located in an outer layer of the pellet (core-shell configuration). In this case, the characteristic dimension, L_p , to be used in Eq. (1) and (3) is the thickness of this layer. Pirard *et al.* [11] studied the oxidation of D-glucose into D-gluconic acid on Pd-Bi/carbon xerogel catalysts in aqueous media; the catalytic species (Bi and Pd) were concentrated in an external layer of the catalyst pellets, as shown by physico-chemical characterization. Mass transport analysis was performed using the appropriate characteristic dimension; it showed that the kinetic measurements had been performed under diffusional regime and the authors concluded that measuring the true kinetic reaction rate implied to choose the experimental conditions within a very small range of values. This finally confirms that the measurement of the specific catalytic activity of catalysts supported on nanostructured carbons such as carbon gels is not an easy task; the choice of the experimental conditions should be subject to high caution.

Note that one could apply the same principles to adsorption; in this case, the reaction rate is replaced by the adsorption rate. Indeed, recent results have shown that the pore texture of carbon gels has the same impact on adsorption processes: the adsorption rate can be increased by selecting a support with appropriate pore texture [12], adsorption sites being more easily reached by the adsorbate molecules. This is quite interesting for purification systems or gas masks, for instance, where the transient adsorption of molecules occurs.

3.2. Electrocatalytic processes

The advantages of carbon gels in heterogeneous catalysis can be transferred to electrochemical devices such as Proton Exchange Membrane fuel cells. The catalytic layer of a PEM fuel cell is composed of Pt/carbon catalyst particles, interparticle voids and ionomer (Nafion®, usually), hot-pressed between a proton-exchange membrane and a gas diffusion layer (GDL) usually made of hydrophobic carbon felt [1]. A catalytic layer of a PEM fuel cell can be seen as a microreactor of heterogeneous catalysis where mass transports are complicated by (i) the presence of two fluid phases (gas and

condensed water) and (ii) the proton transport via the ionomer network. Indeed, to be active, the metal (Pt) catalyst particles must be in contact with the carbon support and connected to the membrane *via* the ionomer. In addition, reactants (H_2 or O_2 , protons and electrons) and water must circulate easily through the catalytic layers; in particular, the catalyst must be reached by the gas through the porous structure of the electrode. Usually, carbon blacks are used as support; however, the packing of the carbon black aggregates, and therefore the pore structure of the catalytic layers, depends on the carbon black nature and on the electrode processing [1]. Typically, at the air-fed cathode, where oxygen, proton and water transports hamper the oxygen reduction reaction, high potential losses due to diffusional limitations offset the cell performance [13]. This is compensated by the use of catalytic layers with high Pt loading, which increases the electrode cost.

The study of mass transport in such systems is not easy because some parameters of the above-written equations are not readily available. For instance, due to the presence of ionomer within the pore texture, the pore size and pore volume is different to that of the pristine carbon gel; this effect is reinforced by the fact that Nafion® swells when humidified, and that some water can condense within the pore texture, reducing further the available pore volume. As a first consequence, the true void fraction accessible to reactants, ε , is difficult to estimate. Concentrations C_e and C_s evolve with the position of the catalyst particles in the MEA, and correlations for the external transport, though available [14], strongly depend on the system geometry. At the moment, diffusional limitations are most often analyzed through the voltage loss analysis of the cell. The total voltage loss of the cell with regard to the reversible H_2/O_2 cell voltage can be decomposed into several components [15]: (i) the kinetic overpotential, η_{ORR} , due to the slowness of the O_2 reduction; (ii) the ohmic losses, η_{Ohm} , due to the resistance of the proton migration through the membrane and the electronic contact resistances; (iii) the mass-transport losses, or 'diffusion overpotential', η_{diff} . In such systems, kinetic and mass transport losses of the anode (H_2 side) can be neglected [15]. One can write:

$$(5) \quad E_{\text{cell}} = E_{\text{rev}} - \eta_{\text{ORR}} - \eta_{\text{Ohm}} - \eta_{\text{diff}}$$

where E_{rev} is the reversible H_2/O_2 cell voltage under the gas pressure and temperature of the cell. The first two contributions to the voltage loss can be measured. Briefly, η_{ORR} is obtained from measurements at low current densities, *i.e.* from data obtained in the near-absence of mass transport limitations and ohmic resistance (Tafel equation) [15]; η_{Ohm} is obtained by measurement of the ohmic resistance of the cell by impedance spectroscopy, performed *in situ*. Finally, all the other terms of Eq. (5) being known, η_{diff} can be deduced by difference. However, the overpotential attributed to mass transport, η_{diff} , remains a black box that actually encloses all the limitation sources that are not attributed to kinetic and ohmic phenomena through direct measurement. In particular it is difficult to determine where mass transport limitations occur in the catalytic layer. This question is still under investigation and remains of high importance in view of electrode optimization.

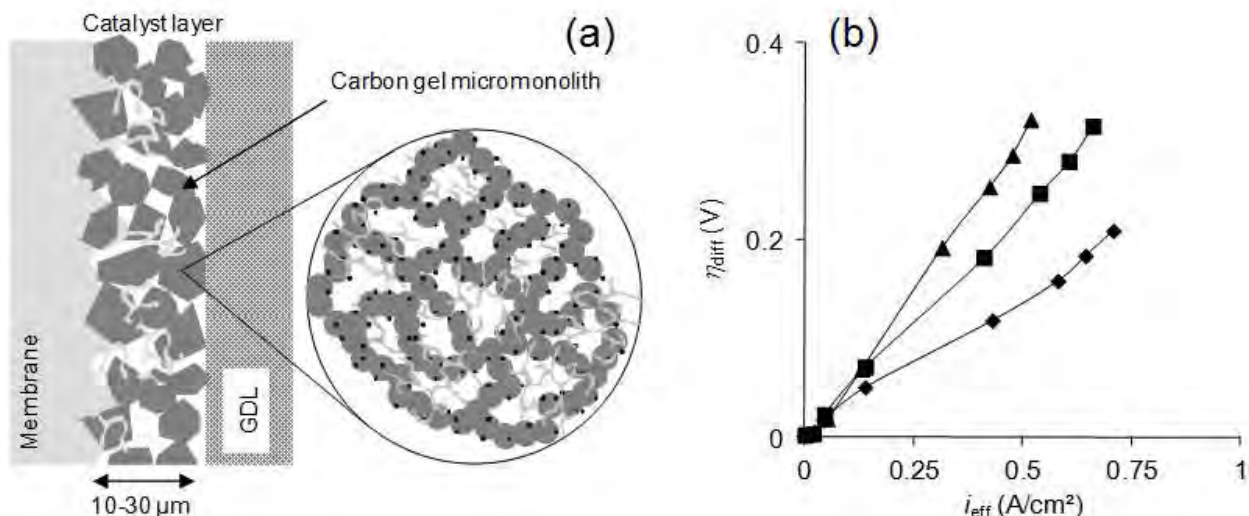


Figure 3. (a) Catalytic layer of a PEM fuel cell with Pt/carbon gel as catalyst; the micromonoliths are made of carbon gel that retains the pore texture of the pristine material, despite grinding. (b) Diffusion overpotential as a function of the current density calculated from measurements in PEM monocell with cathodes prepared from Pt/carbon xerogels of various average meso/macropore size and volume: (p) ~40 nm and 1.0 cm³/g, (n) ~85 nm and 1.8 cm³/g, (u) ~300 nm and 1.9 cm³/g. Adapted from [16].

Figura 3. (a) Capa catalítica de una pila de combustible PEM con Pt/gel de carbón como catalizador; los micromonolitos están hechos de gel de carbón que retiene la textura porosa del material original a pesar de la molienda. (b) Sobrepotencial de difusión en función de la densidad de corriente calculado de las medidas en una monopila PEM con cátodos preparados a partir de Pt/xerogel de carbón de diferentes tamaño medio y volumen de meso/macroporos: (p) ~40 nm and 1.0 cm³/g, (n) ~85 nm and 1.8 cm³/g, (u) ~300 nm and 1.9 cm³/g. Adaptado de [16].

In search for new catalytic layer structures with low diffusion-induced potential losses, carbon gels constitute an interesting alternative to carbon blacks because their meso/macropore texture is totally independent on the electrode processing [16]; besides, the high purity of carbon gels ensures the absence of pollutants inherent to the support origin and detrimental to the electrocatalytic activity. In the electrode structure, the carbon black particle agglomerates are replaced by micromonoliths of carbon gel, which preserves the pores located in-between (Fig. 3a). These materials were used recently to prepare Membrane-Electrode Assemblies (MEAs) for air/H₂ [16-18] or air/methanol PEM fuel cells [19], and were mainly tested at the cathode of a monocell device. In both cases, the pore texture of the carbon gel was found to influence the cell performances: it was possible to decrease the diffusion-induced voltage losses by selecting carbon gels of appropriate pore texture (Fig. 3b). However, many variables influence the final electrode architecture and performance, and the optimization of the pore texture of the carbon support is still an open question.

4. Conclusions

Due to their pore texture versatility, carbon gels are attractive materials as (electro)catalyst supports because an accurate choice of the pore texture can decrease mass transport limitations encountered in operating catalytic processes. However, while few studies pay attention to this problem, the elimination of diffusional limitations is never obvious. As a result, any catalytic system should be first subject to mass transport analysis before any conclusion can be drawn about relationships between the physico-chemical properties and the measured activity of the catalyst. Despite their complex structure, carbon gel-supported catalysts can be studied following classical methods provided that their double-porosity structure is taken into account.

5. Acknowledgements

NJ thanks the F.R.S.-FNRS (Belgium), the Fonds de Recherche Fondamentale Collective and the Ministère de la Région Wallonne (project INNOPEM n°1117490) for funding.

6. References

- Maillard F, Simonov P, Savinova ER. Carbon materials as supports for fuel cell electrocatalysts. In: Carbon Materials for Catalysis, Philippe Serp and José Luis Figueiredo Eds. Wiley, New York, 2009, p. 429-481.
- Elkhatat AM, Al-Muhtaseb S. Adv Mater 2011;23:2887-2903.
- Job N, Théry A, Pirard R, Marien J, Kocon L, Rouzaud JN, Béguin F, Pirard JP. Carbon 2005;43:2481-2494.
- Job N, Gommès CJ, Pirard R, Pirard JP. J Non-Cryst Solids 2008;354:4698-4701.
- Mahata N, Pereira MFR, Suárez-García F, Martínez-Alonso A, Tascón JMD, Figueiredo JL. J Coll Interf Sci 2008;324:150-155.
- Moreno-Castilla C. Carbon gels in catalysis. In: Carbon Materials for Catalysis, Philippe Serp and José Luis Figueiredo Eds. Wiley, New York, 2009, p. 373-400.
- Froment GF, Bischoff KB. Chemical Reactor Analysis and Design, 2nd ed., Wiley, New York, 1990.
- Job N, Heinrichs B, Lambert S, Pirard JP, Colomer JF, Vertruyen B, Marien J. AIChE J 2006;52:2663-2676.

- ⁹ Satterfield CN. Mass Transfer in Heterogeneous Catalysis. Cambridge, MA: MIT Press; 1970.
- ¹⁰ Contreras M, Páez C, Zubizarreta L, Léonard A, Olivera C, Blacher S, Pirard JP, Job N. Carbon 2010;48:3157-3168.
- ¹¹ Pirard SL, Diverchy C, Hermans S, Devillers M, Pirard JP, Job N. Catal Comm 2011;12:441-445.
- ¹² Almazán-Almazán MC, López-Domingo FJ, Domingo-García M, Léonard A, Pérez-Mendoza M, Pirard JP, López-Garzón FJ, Blacher S. Chem Eng J 2011;173:19-28.
- ¹³ Gasteiger HA, Gu W, Makharia R, Mathias MF, Sompalli B. In: Wolf Vielstich, Arnold Lamm and Hubert A. Gasteiger (Eds), Handbook of Fuel Cells – Fundamentals, Technology and Applications, Wiley, Chichester (UK), 2003, Vol. 3, p. 593.
- ¹⁴ Li PW, Zhang T, Wang QM, Schaefer L, Chyu MK. J Power Sources 2003;114:63-69.
- ¹⁵ Gasteiger HA, Kocha SS, Sompalli B, Wagner FT. Appl Catal B 2005;56:9-35.
- ¹⁶ Marie J, Berthon-Fabry S, Chatenet M, Chainet E, Pirard R, Cornet N, Achard P. J Appl Electrochem 2007;37:147-153.
- ¹⁷ Marie J, Chenitz R, Chatenet M, Berthon-Fabry S, Cornet N, Achard P. J Power Sources 2009;190:423-434.
- ¹⁸ Job N, Marie J, Lambert S, Berthon-Fabry S, Achard P. Energ Convers Manage 2008;49:2461-2470.
- ¹⁹ Arbizzani C, Beninati S, Manferrari E, Soavi F, Mastragostino M. J Power Sources 2007;172:578-586.